Eur Phys J A (2005) **24,** s2, 35–38
DOI: 10.1140/epjad/s2005-04-007-1

**EPJ A direct**
**electronic only**

# Transverse spin asymmetry at the A4 experiment

## Experimental results

Sebastian Baunack[a], for the A4-collaboration

Johannes Gutenberg Universität Mainz, Institut für Kernphysik, J.J. Becherweg 45, 55299 Mainz, Germany

Received: 15 October 2004 / Published Online: 8 February 2005


**Abstract.** The A4 collaboration at the MAMI accelerator has measured the transverse spin asymmetry in the cross section of elastic scattering of transversely polarized electrons off unpolarized protons. An azimuthal dependence of the asymmetry has been observed, the amplitudes have been determined as $A_\perp(Q^2 = 0.106\ (\mathrm{GeV/c})^2) = (-8.59 \pm 0.89_{stat} \pm 0.75_{syst}) \cdot 10^{-6}$ and $A_\perp(Q^2 = 0.230\ (\mathrm{GeV/c})^2) = (-8.52 \pm 2.31_{stat} \pm 0.87_{syst}) \cdot 10^{-6}$. $A_\perp$ arises from the imaginary part of the $2\gamma$-exchange amplitude. Our experimentally determined values of $A_\perp$ show that in the intermediate hadronic state not only the ground state of the proton, but also excited states contribute to the asymmetry.

**PACS.** 13.40.Gp Electromagnetic form factors – 11.30.Er Charge conjugation, parity, time reversal, and other discrete – 13.40.-f Electromagnetic processes and properties – 14.20.Dh Properties of protons and neutrons

## 1 Introduction

The A4 collaboration was founded to investigate the asymmetry in the elastic scattering of longitudinally polarized electrons off unpolarized protons. In recent years, theoretical effort has been spent to calculate the asymmetry for transversely polarized electrons [1,2]. The asymmetry arises from the interference between $1\gamma$ and $2\gamma$ exchange (Fig. 1). The calculations take into account the intermediate hadronic state of the $2\gamma$ exchange and might explain the discrepancy between the Rosenbluth separation technique and the polarization transfer method for the dermination of the ratio $G_E^p/G_M^p$ of the electromagnetic form factors of the proton [3].

The A4 segmented lead fluoride ($PbF_2$) calorimeter which covers the full $2\pi$ azimuthal range is an appropiate apparatus to reveal the sinusoidal dependence of the asymmetry on the angle between the electron spin and the scattering plane. We have measured $A_\perp$ at two beam energies 569.31 MeV and 855.15 MeV at scattering angles between $30° \leq \theta \leq 40°$ corresponding to momentum transfers 0.106 $(\mathrm{GeV/c})^2$ and 0.230 $(\mathrm{GeV/c})^2$. In contrast to the parity violation measurements, the transverse electron spin causes physical asymmetries of nonnegligible order in our luminosity monitors. An extensive analysis of these asymmetries, which come from the $2\gamma$ exchange in Møller scattering, has been made in order to understand and control this effect. Our experimentally determined values of $A_\perp$ show that in the intermediate hadronic state not only the ground state of the proton, but also excited states contribute to the physical asymmetry [2].

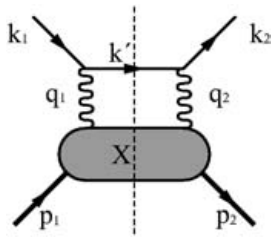


**Fig. 1.** $2\gamma$ exchange

## 2 Experimental setup

The measurement principle is quite simple (Fig. 2): the polarised electron beam hits a hydrogen target and is scattered into the detector which counts the number $N^\pm$ of the elastic scattered particles for two opposite spin directions. The asymmetry is then $A = (N^+ - N^-)/(N^+ + N^-)$.

The measurement took place in the MAMI accelerator facility using the A4-experiment setup, which has been described in detail in [4]. We used an electron beam with an intensity of 20 $\mu A$. Thanks to the polarized electron source using a strained layer GaAs crystal the averaged beam polarization $P_e$ was about 80 %. The spin of the electrons was reversed every 20 ms following a randomly selected pattern, (+ - - +) or (- + + -). The polarization degree of the beam was measured by a Møller polarimeter situated in another experimental hall. The spin of the

[a] comprises part of PhD thesis

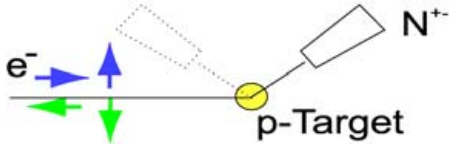


**Fig. 2.** Measurement principle: the polarized electrons hit the liquid hydrogen target. The detector counts the number $N^{\pm}$ of elastic scattered electrons for two opposite spin directions. The scattering angle has been so far $\theta = (35 \pm 5)^{\circ}$. The future measurements will include backward scattering with $\theta = (145 \pm 5)^{\circ}$

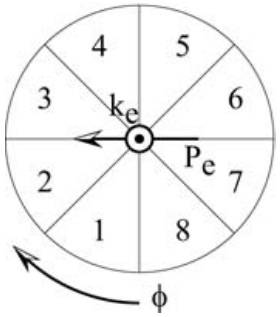


**Fig. 3.** Schematic view of the $PbF_2$ calorimeter from behind. The incoming electron's momentum vector $\mathbf{k}_e$ is pointing out of the paper plane. The momentum vector $\mathbf{k}_{out}$ of the outgoing electron can take all possible $\phi$ values. Both together define the coordinate system. The direction of the electron polarization vector $\mathbf{P}_e$ for the '+' helicity state is indicated by the arrow. $\phi$ is counted as indicated

electrons was put into transverse direction with the help of a Wien filter located between the 100 keV electron source and the injector linac of the accelerator. The exact spin angle was determined by a Møller-Mott polarimeter located at the beam dump. Several monitor and stabilization systems have been installed along the accelerator to minimize beam fluctuations that introduce false asymmetries, such as differences in position, angle and energy for the two helicity states. The electrons were scattered on a 10 cm long liquid hydrogen target. The resulting luminosity is $L \approx 0.5 \cdot 10^{38}\ cm^{-2}s^{-1}$. The luminosity was monitored by eight water-cerenkov monitors put under small scattering angles $\theta = 4.4^{\circ}...8^{\circ}$ covering the full azimuthal range $\phi = 0...2\pi$.

The scattered electrons are detected in a total absorbing calorimeter that consists of 1022 individual lead fluoride ($PbF_2$) crystals placed in 7 rings and 146 rows. It covers scattering angles from $\theta = 30^{\circ}...40^{\circ}$, $\phi = 0...2\,\pi$ and a solid angle $\Delta\,\Omega = 0.64\ sr$. To see the azimuthal angular dependence of the asymmetry, we divide our calorimeter in the analysis into eight sectors, each sector covering $\Delta\Phi \approx 45^{\circ}$. Figure 3 shows our convention of chosen angles and directions.

## 3 Physical asymmetry in Møller scattering

In order to calculate the experimental asymmetry $A_{exp}$, target density fluctuations have to be taken into account.

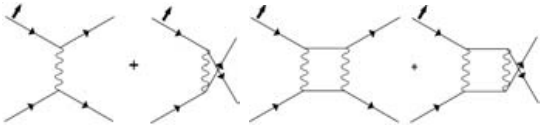

**Fig. 4.** Feynman graphs for Møller scattering: one loop diagrams (*left*) and box diagrams (*right*). The *arrow* indicates the transverse polarisation of the incoming electron. The asymmetry arises from the interference term of the $1\gamma$ and the $2\gamma$-exchange

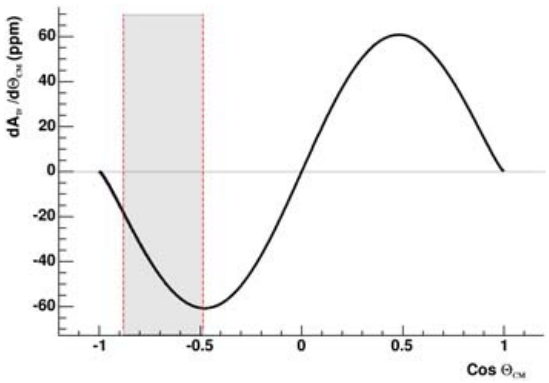


**Fig. 5.** Leading order asymmetry $A_{\perp}^{\text{Møller}}$ in Møller scattering for a beam energy of E=569.31 MeV as a function of the scattering angle $\Theta_{CM}$ in the center of mass system. The two *dashed lines* indicate the polar acceptance of the luminosity monitors

The elastic counts $N^{\pm}$ are normalised to the target density $\rho^{\pm} = L^{\pm}/I^{\pm}$, the ratio of luminosity $L$ and beam current $I$:

$$A_{exp} = \frac{\frac{N^+}{\rho^+} - \frac{N^-}{\rho^-}}{\frac{N^+}{\rho^+} + \frac{N^-}{\rho^-}} \approx \frac{N^+ - N^-}{N^+ + N^-} - \frac{L^+ - L^-}{L^+ + L^-} + \frac{I^+ - I^-}{I^+ + I^-} \tag{1}$$

The approximation is valid up to large asymmetries and certainly for the asymmetries in the A4 experiment. One sees that the asymmetry measured in the luminosity monitors enters linearly into the experimental asymmetry $A_{exp}$. While it is desired to eliminate asymmetries coming from real target density fluctuations, a physical asymmetry in the process of the luminosity measurement would enter false asymmetries into $A_{exp}$. The eight luminosity monitors covering the same $\phi$-ranges as indicated for the calorimeter sectors in Fig. 3 detect mainly Møller scattered electrons. It is known for many years [5] that a $\phi$-depending asymmetry occurs in the Møller scattering of transversely polarized electrons. Most recently, new calculations have been done for the E-158 experiment [6]. Figure 4 shows the one-loop diagrams and the box diagrams for Møller scattering. The physical asymmetry arises from the interference term between these two diagrams. The leading order asymmetry $A_{\perp}^{\text{Møller}}$ is plotted in Fig. 5 for a beam energy of 569.31 MeV as a function of the scattering angle $\Theta_{CM}$ in the center of mass system. The polar acceptance of the luminosity monitors are indicated by the grey box. Since the acceptance is non-symmetric with respect to $\Theta_{CM}$, a nonvanishing physical asymmetry is observable.

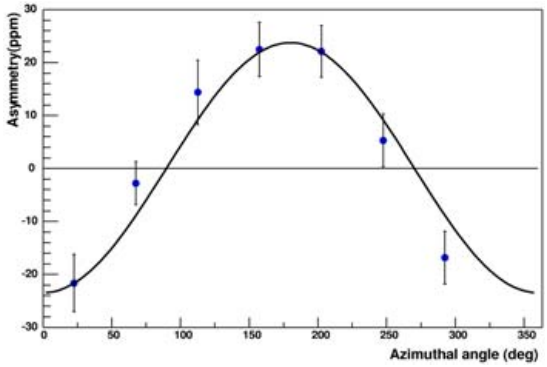


**Fig. 6.** Extracted physical asymmetry in the luminosity monitors as a function of the azimuthal scattering angle $\phi$ at $Q^2$=0.106 (GeV/c)$^2$. The electron spin was almost transverse with $\Phi_s = 85.1°$. The fit gives $A^{Lumi} = (-24.3 \pm 2.9) \cdot 10^{-6}$

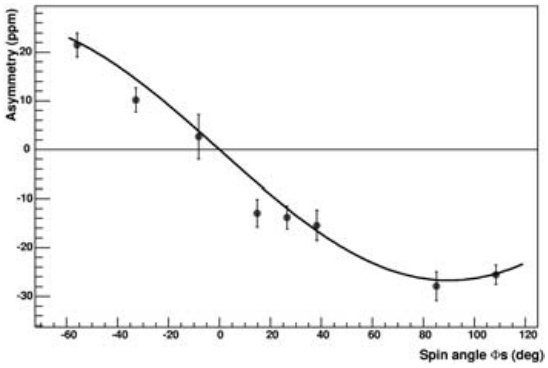


**Fig. 7.** Extracted asymmetry $A^{Lumi}$ of the luminosity monitor as a function of the angle of the electron's spin angle $\Phi_s$ for $Q^2$ =0.106 (GeV/c)$^2$. The fit to the data gives $A_\perp^{\mathrm{Lumi}} = (-26.7 \pm 1.3) \cdot 10^{-6}$

An experimental verification and systematic check of the asymmetries in the luminosity monitors is possible during a spin rotation measurement. The Wien filter rotates the spin of the electrons from longitudinal to transverse direction in discrete steps by applying various currents. The corresponding spin angles are determined by the dump polarimeter. According to the spin angle a change in size and sign of the azimuthal dependence of the asymmetries in the luminosity monitors should be observable. Figure 6 shows the observed asymmetries for an almost transverse spin angle $\Phi_s = 85.1°$ and $Q^2$ =0.106 (GeV/c)$^2$. The sinusoidal behaviour is obvious. The amplitude is $A^{\mathrm{Lumi}} = (-24.3 \pm 2.9) \cdot 10^{-6}$. Measurements at various spin angles $\Phi_s$ of $A^{\mathrm{Lumi}}(\Phi_s)$ make a fit possible to determine $A_\perp^{\mathrm{Lumi}}$. We performed such an analysis for both of our so far applied momentum transfers. Figure 7 shows the result for our low $Q^2$ value. Due to target density fluctuations and shorter measurement times, the result for the higher $Q^2$ value has a larger uncertainty.

Table 1 gives the results of the NLO calculations for $A_\perp^{\mathrm{Møller}}$ and our observed asymmetries $A_\perp^{\mathrm{Lumi}}$ in the luminosity monitors. For a comparison of these values one has to keep in mind that the luminosity monitors do not only see Møller electrons, but a certain 'dilution' of elastic scattered electrons. We understand qualitatively the occuring asymmetries. For a normalisation of the elastic counts, the luminosity signals have to added $\Phi$-symmetrically, since the physical asymmetry in Møller scattering then averages out.

**Table 1.** NLO calculation for the transverse spin asymmetry $A_\perp^{\mathrm{Møller}}$ in Møller scattering and comparison with the observed asymmetries $A_\perp^{\mathrm{Lumi}}$ in the luminosity monitors

| $Q^2$ | $A_\perp^{\mathrm{Møller}}$ NLO calc. | $A_\perp^{\mathrm{Lumi}}$ exp. |
|---|---|---|
| 0.106 (GeV/c)$^2$ | $-29.6 \cdot 10^{-6}$ | $(-26.7 \pm 1.3) \cdot 10^{-6}$ |
| 0.230 (GeV/c)$^2$ | $-16.6 \cdot 10^{-6}$ | $(-23.3 \pm 4.3) \cdot 10^{-6}$ |

**Table 2.** Beam parameters for momentum transfer $Q^2$=0.230 (GeV/c)$^2$ achieved within 47 hours and $Q^2$=0.106 (GeV/c)$^2$ßachieved within 54 hours of pure data taking

| Parameter | 0.23 $(GeV/c)^2$ | 0.11 $(GeV/c)^2$ |
|---|---|---|
| $A_I$ | $(2.5 \pm 0.6)$ ppm | $(0.4 \pm 1.4)$ ppm |
| $\Delta x$ | $(15.1 \pm 3.4)$ nm | $(157.0 \pm 150.0)$ nm |
| $\Delta y$ | $(-126.7 \pm 18.0)$ nm | $(-504.3 \pm 43.7)$ nm |
| $\Delta x'$ | $(5.4 \pm 0.8)$ nrad | $(20.5 \pm 12.9)$ nrad |
| $\Delta y'$ | $(21.5 \pm 3.0)$ nrad | $(45.4 \pm 3.9)$ nrad |
| $\Delta E$ | $(0.2 \pm 0.3)$ eV | $(41.4 \pm 2.6)$ eV |

## 4 Determination of transverse asymmetry $A_\perp$

For the determination of the physical asymmetry we use the same technique that we already used in the parity violating case [4]. The experimental measured asymmetry $A_{exp}(\Phi_i)$ of each sector $i$ can be written as the sum of the physical asymmetry $A_{phys}(\Phi_i)$ and the helicity correlated false asymmetries $A_j$, $j = 1..6$:

$$A_{exp}(\Phi_i) \;=\; P \;\cdot\; A_{phys}(\Phi_i) \;+\; \sum_{i=1}^{6} a_i \; X_i \qquad (2)$$

with $P$ the beam polarisation, $X_1$ the asymmetry in beam current, $X_2$, $X_3$ the differences in horizontal and vertical position, $X_3$, $X_4$ differences in horizontal and vertical angle and $X_6$ difference in beam energy. We determine the coefficients $a_i$ via a multiple linear regression out of the asymmetry data itself. Thanks to the stabilisation systems, the quantities $X_i$ could be kept small. Table 2 shows the achieved values for the two momentum transfers. We have 47 hours beam data for E=569.31 MeV and 54 hours for E=855.15 MeV, corresponding to a number of elastic events of $N_{tot} = 3.9 \cdot 10^{12}$ and $N_{tot} = 6.3 \cdot 10^{11}$ respectively. Figure 8 show the physical asymmetries as a function of the azimuthal scattering angle $\Phi$. At the time of the

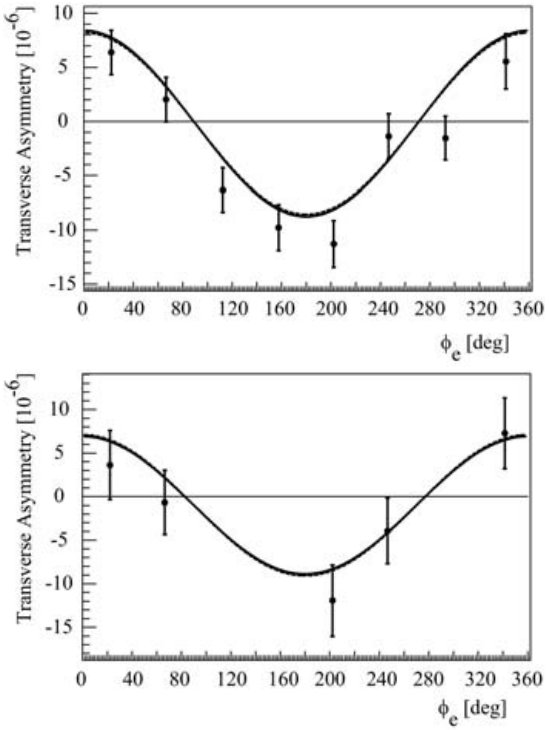


**Fig. 8.** Extracted physical asymmetries for the eight sectors of the calorimeter for $Q^2$=0.106 (GeV/c)$^2$ (*upper plot*) and $Q^2$=0.230 (GeV/c)$^2$

0.230 (GeV/c)$^2$-measurement, only sectors 1, 2, 5, 6 and part of sector 8 have been equipped with detectors. We fit to the data an averaged function $A_\perp^m$ which takes into account that each sector covers about 45° in the azimuthal range:

$$A_\perp^m(\phi) = \int_{\phi-\pi/8}^{\phi+\pi/8} A_\perp \cos\phi' d\phi' = 0.765 A_\perp \cos\phi \qquad (3)$$

Applying dead time corrections and corrections for aluminum dilution from the target entry and exit windows, we obtain:

$$A_\perp(Q^2 = 0.11) = (-8.59 \pm 0.89_{stat} \pm 0.75_{syst}) \cdot 10^{-6}$$
$$A_\perp(Q^2 = 0.23) = (-8.52 \pm 2.31_{stat} \pm 0.87_{syst}) \cdot 10^{-6}$$

The first error represents the statistical uncertainty and the second error the systematic error.

## 5 Conclusion and outlook

A comparison of our measured values of $A_\perp$ with model calculations from [2] shows that the size of the observed asymmetries can not be explained if one takes into account only the elastic contribution to the intermediate nucleon state (Fig. 9). Even at our low $Q^2$ nucleon resonances play an important role. For the future we plan an extensive measurement program at various energies under forward and backward angles on hydrogen as well as on deuterium (Table 3 and Table 4).

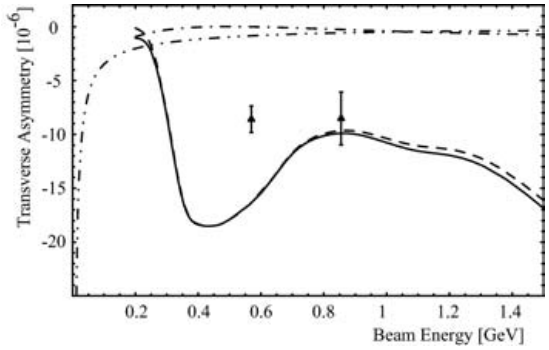


**Fig. 9.** Our extracted asymmetries $A_\perp$ compared with model calculations from [2] as a function of the beam energy. For the *dashed dotted line* the intermediate nucleon state has been the ground state only. The *dashed line* represents the contribution of all possible $\pi$N intermediate states. The *solid line* is the sum of both contributions

**Table 3.** Projected measurements for transverse single spin asymmetries $A_\perp$ with hydrogen and deuterium under forward angles ($\Theta = (35 \pm 5)°$)

| $E_e$ [$MeV$] | $\delta A_\perp^p$ [$ppm$] | hours proton | $\delta A_\perp^D$ [$ppm$] | hours deuteron | $\delta A_\perp^n$ [$ppm$] |
|---|---|---|---|---|---|
| 300 | 0.5 | 20 | 0.5 | 20 | 20 |
| 420 | 0.5 | 40 | 0.5 | 35 | 11 |
| 570 | 0.5 | 90 | 0.5 | 70 | 7 |
| 854 | 0.5 | 300 | 0.5 | 220 | 4 |
| 1200 | 1 | 260 | 1 | 180 | 6 |
| 1500 | 2 | 180 | 2 | 120 | 11 |

**Table 4.** Projected measurements for transverse single spin asymmetries $A_\perp$ with hydrogen and deuterium under backward angles ($\Theta = (145 \pm 5)°$)

| $E_e$ [$MeV$] | $\delta A_\perp^p$ [$ppm$] | hours proton | $\delta A_\perp^D$ [$ppm$] | hours deuteron | $\delta A_\perp^n$ [ppm] |
|---|---|---|---|---|---|
| 300 | 3 | 90 | 2 | 130 | 10 |
| 420 | 3 | 230 | 2 | 320 | 10 |
| 570 | 4 | 370 | 3 | 390 | 13 |
| 854 | 8 | 490 | 7 | 380 | 28 |

## References

1. P.A.M. Guichon, M. Vanderhaeghen: Phys. Rev. Lett. **91**, 142303 (2003)
2. B. Pasquini, M. Vanderhaeghen: hep-ph/0405303 (2003)
3. J. Arrington: nucl-ex/0408020
4. F.E. Maas et al.: Phys. Rev. Lett. **93**, 022002 (2004)
5. A.O. Barut, C. Fronsdal: Phys. Rev. **120**, 1871 (1960)
6. L. Dixon, M. Schreiber: Phys. Rev. D **69**, 113001 (2004)